Stability of Bose-Einstein condensates in two-dimensional optical lattices

Zhu Chen (陈竹) and Biao Wu (吴飙)
Institute of Physics, Chinese Academy of Sciences, Beijing 100190, People's Republic of China
(Received 26 October 2009; revised manuscript received 3 December 2009; published 13 April 2010)

Both Landau instability and dynamical instability of Bose-Einstein condensates in moving two-dimensional optical lattices are investigated numerically and analytically. Phase diagrams for both instabilities are obtained numerically for different system parameters. These phase diagrams show that the Landau instability does not depend on direction for weak lattices while the dynamic instability is direction dependent. These features are explained analytically.

DOI: 10.1103/PhysRevA.81.043611 PACS number(s): 03.75.Kk, 05.30.Jp, 37.10.Jk, 47.37.+q

I. INTRODUCTION

Bose-Einstein condensates (BECs) in optical lattices have been attracting much attention for their rich physics and the possibility of precise and flexible control of system parameters [1,2]. Extensive work, both experimental and theoretical, has been done on such systems from various perspectives. They include fundamental quantum phenomena such as superfluidity [3–7], quantum phase transition [8–10], and quantum vortex formation [11]; effects long predicted but not cleanly observed in solid-state systems, for example, Bloch oscillations [12,13] and Landau-Zener tunneling [14–16]; and nonlinear effects such as various kinds of instabilities [4,17–22] and gap solitons [23,24].

In this article we focus on the superfluidity and instabilities of BECs in optical lattices. They are the basic properties of superfluids and therefore of fundamental interest. In free space, there exists the Landau criterion for superfluids; that is, there is a critical speed above which any small disturbances lead to a drop in energy and thus the breakdown of superfluidity [25]. A similar question can be asked for a BEC in a moving optical lattice: What is the critical speed of the lattice above which the system loses its superfluidity [26]? Such a breakdown of superflow is called Landau instability or energetic instability [27]. Interestingly, another type of instability, dynamical instability, exists in the preceding periodic system. This instability can be viewed as a new way of loss of superfluidity. As demonstrated in experiment [21], the dynamical instability has a much shorter time scale and manifests itself in the form of fragmentation of the BEC.

So far, most of theoretical work concerns only BECs in one-dimensional (1D) optical lattices [28–35]. Studies in two- or three-dimensional optical lattices are scarce. In the present article we study both Landau and dynamical instabilities of BECs in two-dimensional (2D) optical lattices, both numerically and analytically. We obtain the stability phase diagrams numerically. We find that the Landau instability is independent of directions for weak optical lattices while the dynamical instability is direction dependent. We manage to explain all the salient features in our numerical results with analytical results.

The article is organized as follows. In Sec. II, we briefly introduce our theoretical model and the methods that we use to study the instabilities. In Sec. III, the results for Landau instability are presented and discussed. In Sec. IV, we present and analyze the results for dynamical instability. Finally, in Sec. V, we discuss the results and conclude.

II. MODEL AND METHODS

A. Mean-field theory of Bose-Einstein condensates

We focus on the situation where the BEC system can be well described by a mean-field macroscopic wave function ψ. The wave function is governed by the following Hamiltonian:

$$\mathcal{H} = \int d^3\vec{r}\,\left\{\psi^*\left[-\frac{1}{2}\nabla^2 + V_{\text{latt}}\right]\psi + \frac{c}{2}|\psi|^4\right\}. \quad (1)$$

In our case, the external potential is a 2D optical lattice created by four laser beams and has the form

$$V_{\text{latt}} = \upsilon(\cos x + \cos y), \quad (2)$$

where υ characterizes the strength of the optical lattice. In Eq. (1), all of the variables are scaled to be dimensionless by the system's basic parameters, following the scheme of Ref. [4].

The Gross-Pitaevskii (GP) equation is obtained by the variation of the Hamiltonian, $i\partial\psi/\partial t = \delta H/\delta\psi^*$,

$$i\frac{\partial\psi}{\partial t} = -\frac{1}{2}\nabla^2\psi + V_{\text{latt}}\psi + c|\psi|^2\psi. \quad (3)$$

Generally speaking, the preceding periodic wave equation has Bloch wave solutions, which can be written as $\psi(\vec{r},t) = e^{i\vec{k}\cdot\vec{r}-i\mu t}\phi_{\vec{k}}(\vec{r})$. The wave vector $\vec{k}$ marks different eigenstates and $\phi_{\vec{k}}(\vec{r})$ is a periodic function with the same period as the potential. The band index is ignored here since we consider only the lowest Bloch band.

B. Analysis of linear stability

The linear stability of a system is about how the system responses to a small disturbance. The dynamical response of a BEC to a perturbation is governed by the Bogoliubov equation [27],

$$i\frac{\partial}{\partial t}\begin{pmatrix}u_{\vec{k}}\\ v_{\vec{k}}\end{pmatrix} = \sigma_z M_{\vec{k}}(\vec{q})\begin{pmatrix}u_{\vec{k}}\\ v_{\vec{k}}\end{pmatrix}, \quad \sigma_z = \begin{pmatrix}I & 0\\ 0 & -I\end{pmatrix}, \quad (4)$$

with the perturbation matrix

$$M_{\vec{k}}(\vec{q}) = \begin{pmatrix}\mathcal{L}(\vec{k}+\vec{q}) & c\phi_{\vec{k}}^2\\ c\phi_{\vec{k}}^{*2} & \mathcal{L}(-\vec{k}+\vec{q})\end{pmatrix} \quad (5)$$

and

$$\mathcal{L}(\vec{k}') = -\tfrac{1}{2}(\nabla + i\vec{k}')^2 + V_{\text{latt}}(\vec{r}) - \mu + 2c|\phi_{\vec{k}}|^2, \quad (6)$$

where $\vec{k}$ denotes the wave vector of Bloch states and $\vec{q}$ represents the mode of perturbation.

We can see from Eq. (4) that once the matrix $\sigma_z M_{\vec{k}}$ has complex eigenvalues, which appear always in conjugate pairs, certain modes of perturbation grow exponentially in time. This means that the superflow breaks down and the system becomes dynamically unstable.

The real eigenvalues of $\sigma_z M_{\vec{k}}$ can be grouped into two. For the first group, the eigenvectors have positive norm while the eigenvectors in the second group have negative norm. Only the first group are physical and they are called phonon modes [4]. When the eigenvalues of $\sigma_z M_{\vec{k}}$ for all the phonon modes are positive, the Bloch wave $\phi_{\vec{k}}$ is a local energy minimum and it represents a superflow. Otherwise, $\phi_{\vec{k}}$ is an energy saddle point and the system in this state suffers Landau instability.

Note that, generally, people use the eigenvalues of $M_{\vec{k}}$ to determine the Landau instability in literature, instead of $\sigma_z M_{\vec{k}}$ [4]. As shown in the Appendix, these two criteria are equivalent. As a result, one only needs to diagonalize $\sigma_z M_{\vec{k}}$ numerically to investigate the onset of both instabilities; this reduces the numerical computation load by half. However, analytically, we find that it is more convenient to use $M_{\vec{k}}$ to study Landau instability. The reason is that if $\sigma_z M_{\vec{k}}$ is used, two sets of criteria are obtained: one from singling out the phonon modes and the other from the phonon having positive eigenvalues. The criterion of Landau instability is the combination of the two. This turns out to be much more complicated than using $M_{\vec{k}}$. So, in this work we still use $M_{\vec{k}}$ in our analysis to determine the Landau instability.

III. LANDAU INSTABILITY

A. Numerical results

We have numerically computed the eigenvalues of the matrix $\sigma_z M_{\vec{k}}(\vec{q})$ based on which instability of the system—Landau or energetic—can be determined. The results are summarized in the stability phase diagrams shown in Fig. 1. We are interested in two features of the diagrams: the shape of the stability boundary and the location of the boundary, or the critical value $\vec{k}_c$ where the Landau instability begins to appear.

(i) When the lattice strength is weak, the boundary of the Landau instability appears as an arc (see the left column of Fig. 1). This indicates that the critical value of $\vec{k}$ for the Landau instability is independent of directions.

(ii) We notice that, similar to the 1D results [4], the unstable region shrinks with increasing nonlinear interaction. This implies that the system becomes more robust against long-wavelength disturbance. In particular, the dependence of the stability boundary on the lattice strength varies as the nonlinear interaction c changes. In Fig. 2, we have plotted how the critical value k_{xc} along the x direction changes with the lattice strength v. It is clear from the figure that k_{xc} decreases with v for large c while it increases with v for small c. It also appears that k_{xc} approaches $1/4$ when v becomes very large.

In the following sections, we try to explain these features both qualitatively and quantitatively.

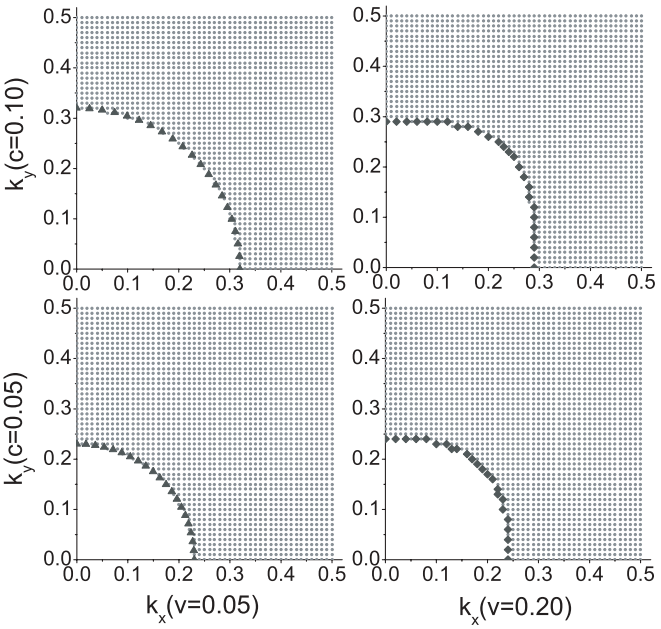

FIG. 1. Phase diagrams of Landau instability for a BEC in a 2D optical lattice, with k_x, k_y being the wave numbers of BEC Bloch states. The shaded region is where Landau instability occurs. The solid triangles in the left column are the boundaries obtained with the effective mass theory and the solid diamonds in the right column represent the boundaries obtained with the hydrodynamical analysis. Both theoretical results agree very well with our numerical results.

B. Weak lattice limit

The direction-independent behavior seen in the first column of Fig. 1 is easily understandable from two aspects. First, the critical velocity of a BEC in free space does not depend on its direction; weak lattice, which can be treated as perturbation, should not bring qualitative changes. Second, the Landau instability is determined by long-wavelength perturbations, which are insensitive to the lattice structure.

Here we attempt to provide a quantitative understanding through a simple effective mass theory. When the lattice is weak, the effect of periodic potential can be absorbed into an effective mass m^*. In other words, the system can be mapped to an effective one in which the condensate moves in free space

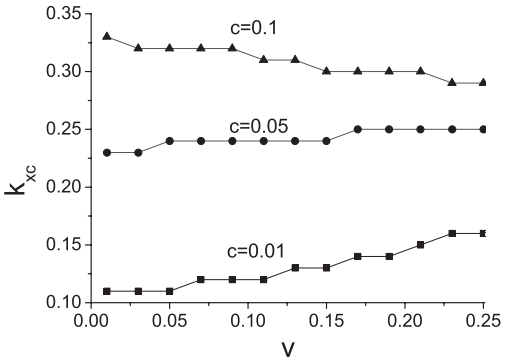

FIG. 2. The critical value of $\vec{k}$ along the x direction for the onset of Landau instability as a function of lattice strength v. The results are for three representative values of interaction strengths. We set $k_y = 0$ for simplicity.

with the renormalized dispersion $E(\vec{k}) \approx (\hbar\vec{k})^2/2m^*$. Thus, we can use the method used by Landau to analyze the condition for the onset of Landau instability and find the critical velocity as follows [26]:

$$v_t = \frac{m^*}{m}u_0 = \frac{\hbar k_{xc}}{m}, \tag{7}$$

where u_0 is the sound velocity of a BEC in a Bloch state at $\vec{k} = 0$ and k_{xc} is the corresponding wave number. If we define $\vec{v}_g = m\vec{v}/m^*$, then the preceding condition for the appearance of Landau instability can be rewritten as

$$v_g > u_0. \tag{8}$$

This criterion has the same form as the Landau criterion of superfluidity in free space.

Since the sound velocity is direction independent, the boundary of the Landau instability region should also be direction independent. Having computed different sound velocities according to the formula in Ref. [36], we obtain the corresponding critical wave numbers with Eq. (7). These results are plotted as solid triangles and compared with our previous numerical results in the first column of Fig. 1. The perfect match indicates the validity of the preceding effective mass theory.

C. Tight-binding approximation

With a strong lattice, the condensate can be regarded as a chain of weakly linked small condensates localized in different potential wells. In this case, the system goes into the tight-binding regime. In the tight-binding approximation, we expand the macroscopic wave function as $\psi(\vec{r},t) = \sum_{n,m}\psi_{n,m}(t)w_{n,m}(\vec{r})$, where $w_{n,m}$ is the Wannier function for the (n,m)th site of the lattice. With this expansion, the dimensionless GP equation (3) is transformed into a set of discretized equations [37],

$$i\frac{\partial\psi_{n,m}}{\partial t} = -K(\psi_{n+1,m} + \psi_{n-1,m} + \psi_{n,m+1} + \psi_{n,m-1}) + \chi|\psi_{n,m}|^2\psi_{n,m}, \tag{9}$$

where $K = -\frac{1}{4\pi^2}\int d\vec{r}\sum_{\langle n,m,n',m'\rangle}[\frac{1}{2}\vec{\nabla}w^*_{n,m}\cdot\vec{\nabla}w_{n',m'} + w^*_{n,m}V_{\rm latt}w_{n',m'}]$ and $\chi = \frac{c}{4\pi^2}\int d\vec{r}|w_{n,m}|^4$. The symbols $\langle\ \rangle$ denote the nearest neighbors.

The perturbation matrix for the above model is

$$M_{\vec{k}}(\vec{q}) = \begin{pmatrix} \mathcal{L}(\vec{k}+\vec{q}) & \chi \\ \chi & \mathcal{L}(-\vec{k}+\vec{q}) \end{pmatrix}, \tag{10}$$

with

$$\mathcal{L}(\vec{k}+\vec{q}) = \chi + 4K\sin(\pi q_x + 2\pi k_x)\sin(\pi q_x) + 4K\sin(\pi q_y + 2\pi k_y)\sin(\pi q_y). \tag{11}$$

When Landau instability happens, $M_{\vec{k}}(\vec{q})$ is no longer positive definite. From this, we obtain two set of conditions. One is

$$\cos(2\pi k_x) < 0 \quad \text{or} \quad \cos(2\pi k_y) < 0; \tag{12}$$

the other is

$$4K[\sin^2(\pi q_x)\cos(2\pi k_x) + \sin^2(\pi q_y)\cos(2\pi k_y)]^2 - K[\sin(2\pi q_x)\sin(2\pi k_x) + \sin(2\pi q_y)\sin(2\pi k_y)]^2 + 2\chi[\sin^2(\pi q_x)\cos(2\pi k_x) + \sin^2(\pi q_y)\cos(2\pi k_y)] < 0. \tag{13}$$

Considering that Landau instability is caused by long-wavelength disturbance, we simplify inequality (13) by taking the limit $q_{x,y} \to 0$ and neglecting the second order quantities. We obtain

$$q_x^2\cos(2\pi k_x) + q_y^2\cos(2\pi k_y), \quad \frac{-2K}{\chi}[q_x\sin(2\pi k_x) + q_y\sin(2\pi k_y)]^2 < 0. \tag{14}$$

We finally arrive at the criterion for Landau instability. There are three sets.

(i)

$$\cos(2\pi k_x) < \frac{2K}{\chi}\sin^2(2\pi k_x); \tag{15}$$

(ii)

$$\cos(2\pi k_y) < \frac{2K}{\chi}\sin^2(2\pi k_y); \tag{16}$$

(iii)

$$\cos(2\pi k_i) > \frac{2K}{\chi}\sin^2(2\pi k_i), \quad (i = x, y), \quad \frac{2K}{\chi}[\sin^2(2\pi k_x)\cos(2\pi k_y) + \sin^2(2\pi k_y)\cos(2\pi k_x)] > \cos(2\pi k_x)\cos(2\pi k_y). \tag{17}$$

Landau instability occurs when any set of these criteria is satisfied.

The preceding criteria are not the direct generalization of its 1D correspondence [27]. Criterion (17) arises as the effect of higher dimension. It is clear from the preceding criteria that deep in the tight-binding regime, the border of Landau instability is at $k_x = k_y = 1/4$.

The general trends seen in Fig. 2 can now be understood. In a weak lattice limit, we should have $k_{xc} = s \sim \sqrt{c}$. Therefore, depending on the value of c, k_{xc} can either be larger or smaller than $1/4$, which is the critical value at the limit of deep tight binding. As the lattice strength increases and the system enters the deep tight-binding regime, the k_{xc}-v curves approach $1/4$ either from above or from below. This is exactly what we see in Fig. 2.

D. Hydrodynamic analysis of long-wave disturbance

We have presented analytical results for both weak and strong lattice limits, which are found to agree very well with numerical results. In general, the hydrodynamic approach is applicable since the onset of the Landau instability occurs at long wavelengths. We follow the work of Machholm [38,39] and Taylor [40].

We work with the average particle density $\overline{n}(\mathbf{r})$ and an average phase, where the averages are to be taken over a volume having linear dimensions much greater than the lattice

spacing but still much smaller than the wavelength of the disturbance. We assume the energy density is given as follows:

$$E = \int d\vec{r}\, \widetilde{E}(\overline{n}(\vec{r}), \overline{\mathbf{k}}(\vec{r})). \tag{18}$$

Here $\widetilde{E}$ is the energy of a uniform system having a wave vector $\vec{k}$ and particle density n.

We denote changes in local density by δn and those in the wave vector by $\delta\mathbf{k}$. After expanding the energy functional around the original state and ignoring the higher-order terms, we find the energy deviation

$$\delta E = \int d\vec{r} \left\{ \frac{1}{2} \left[\frac{\partial \mu}{\partial n} \delta n^2 + \widetilde{E}_{k_x,k_x} \delta k_x^2 + \widetilde{E}_{k_y,k_y} (\delta k_y)^2 + 2\, \widetilde{E}_{k_x,k_y} \delta k_x \delta k_y + 2\delta n \left(\frac{\partial \mu}{\partial k_x} \delta k_x + \frac{\partial \mu}{\partial k_y} \delta k_y \right) \right] \right\}, \tag{19}$$

where $\mu = \frac{\partial \widetilde{E}}{\partial n}$ and $E_{k_i,k_j} = \frac{\partial^2 \widetilde{E}}{\partial k_i \partial k_j}$. The first-order terms have been dropped because they vanish given the total number of particles and the phase of the wave function at the boundaries are fixed [38]. Once the quadratic order terms becomes negative, which means that perturbation helps to lower the system's energy, Landau instability appears. We look into the preceding equation and seek the conditions for $\delta E < 0$.

With the given fact that $\frac{\partial \mu}{\partial n} > 0$ and treating the right-hand side of Eq. (19) as a quadratic function of δn, we arrive at the following inequality:

$$\frac{\partial \mu}{\partial n} \left[\widetilde{E}_{k_x,k_x} \delta k_x^2 + \widetilde{E}_{k_y,k_y} \delta k_y^2 + 2 \widetilde{E}_{k_x,k_y} \delta k_x \delta k_y \right] < \left[\frac{\partial \mu}{\partial k_x} \delta k_x + \frac{\partial \mu}{\partial k_y} \delta k_y \right]^2. \tag{20}$$

We focus on inequality (20) and now treat it as a quadratic function of δk_x. We also notice the symmetry of the preceding inequality about δk_x and δk_y. Performing a similar analysis as previously described, the general conditions for Landau instability are derived finally as follows:

$$\left(\frac{\partial \mu}{\partial k_x} \right)^2 > \frac{\partial \mu}{\partial n} \widetilde{E}_{k_x,k_x}; \tag{21}$$

$$\left(\frac{\partial \mu}{\partial k_y} \right)^2 > \frac{\partial \mu}{\partial n} \widetilde{E}_{k_y,k_y}; \tag{22}$$

and

$$\left(\frac{\partial \mu}{\partial k_i} \right)^2 < \frac{\partial \mu}{\partial n} \widetilde{E}_{k_i,k_i}, \quad (i = x, y),$$
$$\frac{\partial \mu}{\partial n} \left(\widetilde{E}_{k_x,k_y}^2 - \widetilde{E}_{k_x,k_x} \widetilde{E}_{k_y,k_y} \right) > 2 \frac{\partial \mu}{\partial k_x} \frac{\partial \mu}{\partial k_y} \widetilde{E}_{k_x,k_y} - \left(\frac{\partial \mu}{\partial k_x} \right)^2 \widetilde{E}_{k_y,k_y} - \left(\frac{\partial \mu}{\partial k_y} \right)^2 \widetilde{E}_{k_x,k_x}. \tag{23}$$

Sufficient conditions for Landau instability are that any one of conditions (21)–(23) is satisfied.

Actually, both the effective mass theory and the tight-binding criteria can be reproduced from these hydrodynamical criteria and the hydrodynamical approach indeed provides us with a unified prescription of Landau instability. We also have computed the boundaries of Landau instability according to these hydrodynamical criteria and compared them with our numerical results. The comparison is shown in the second column of Fig. 1 with the solid diamonds representing the theoretical results, which shows a perfect match with the numerical results.

IV. DYNAMICAL INSTABILITY

A. Numerical results

We numerically diagonalize the matrix $\sigma_z M_{\vec{k}}$ and determine whether the system is dynamically stable from its eigenvalues: Once there exists any complex eigenvalue, the system becomes dynamically unstable. The results are summarized in the dynamical instability phase diagrams shown in Fig. 3.

Similar to the situation of Landau instability, increasing interaction strength leads to obvious shrinking of the region of dynamical instability. Also, stronger lattice strength causes the critical values of k_x and k_y for the onset of instability approach 1/4 for the tight-binding regime.

The obvious difference from Landau instability is the critical value of $\vec{k}$ for dynamical instability depends on directions, as clearly shown in Fig. 3. This is partially due to that dynamical instability is induced by short-wave disturbance; thus, the configuration of the lattice potential intervenes and plays an important role. Another point that must be noticed is the shape of the stability boundary. For our numerical calculation precision and the range of the parameters that we considered, we find that almost all phase boundaries can be divided into three sections: one section parallel to the k_x direction, another section parallel to the k_y direction, and the third section perpendicular to the diagonal line ($k_x = k_y$). We also find that when nonlinear interaction is weak, the critical

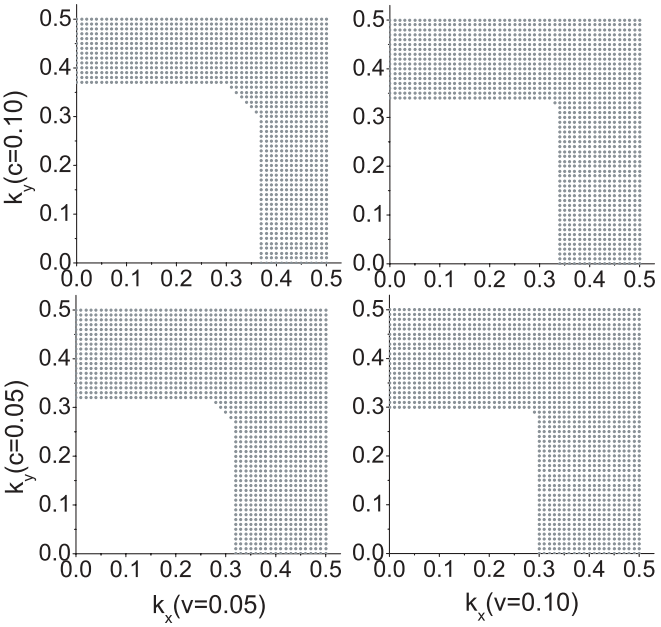

FIG. 3. Dynamical instability phase diagram of a BEC in a 2D optical lattice under different parameters. The shaded regions represent dynamical instability. k_x and k_y are Bloch wave numbers along x and y direction, respectively.

wave vector of the onset of dynamical instability along either x or y direction almost equals its 1D counterpart with the same parameters. In the following, we shall analyze these interesting features one by one.

B. Reduction to 1D dynamics

The two parallel sections of the stability boundaries in Fig. 3 strongly suggest that the x and y motions of the 2D system are decoupled. Therefore, we decompose the 2D Bloch state into two independent 1D motions

$$\psi \simeq \psi_x \psi_y, \tag{24}$$

where $\frac{1}{2\pi}\int_0^{2\pi}|\psi_x|^2 dx = \frac{1}{2\pi}\int_0^{2\pi}|\psi_y|^2 dy = 1$. Plugging Eq. (24) into Eq. (3) and integrating along the y direction, we obtain

$$-\frac{1}{2}\frac{\partial^2}{\partial x^2}\psi_x + v\cos(x)\psi_x + c'|\psi_x|^2\psi_x = \mu'\psi_x, \tag{25}$$

with $c' = \frac{c}{2\pi}\int_0^{2\pi}|\psi_y|^4 dy$. In this way, the 2D motion is decomposed to two orthogonal 1D motions, each with its renormalized nonlinear parameters. The two parallel sections of the boundary are just the result of this decoupled motion. By assuming ψ_y as the solution of the 1D GP function, we have computed the values of c' under typical parameters and found that it does not change much. This implies that the critical values of $k_{x,y}$ for the 2D dynamical instability are close to the ones for the 1D system with the same parameters. A comparison is shown in Table. I.

Similarly, the section perpendicular to the diagonal line suggests an effective 1D motion along the diagonal direction. To see this more clearly, we introduce a new set of coordinates x'-y', with the relations $x' = (x+y)/2$, $y' = (-x+y)/2$, which is equivalent to rotating the former coordinates counterclockwise 45° and rescaling them by $\sqrt{2}/2$. In the rotated frame, the potential possesses a different configuration, and Eq. (3) becomes

$$i\frac{\partial\psi}{\partial t} = -\frac{1}{2}\nabla^2\psi + 4v\cos(x')\cos(y')\psi + 2c|\psi|^2\psi. \tag{26}$$

From this equation, the dynamical instability phase diagram in x'-y' coordinates can be obtained and is shown in Fig. 4. A section parallel to k'_y, which corresponds to the diagonal 1D motion in the x-y coordinates, is clearly seen. Note that Figs. 3 and 4 are related by $k_{x'} = k_x + k_y$ and $k_{y'} = k_y - k_x$. Note that when we talk about Fig. 3, we refer to its lower left subgraph, which has the same parameters as Fig. 4.

We have numerically seen that it is also true in 2D that the onset of dynamical instability of the usual Bloch states coincides with the appearance of period-doubled states with the same energy and wave number [39], which can be understood in terms of four-wave mixing [27,41–43]. For period-doubled states corresponding to the section parallel to the axes, period doubling occurs in either the x or the y direction, while, for the section parallel to the diagonal direction, period doubling occurs in both the x and the y directions.

TABLE I. Critical values of k_x of dynamical instability of a BEC in a 2D optical lattice and the corresponding k 1D motion.

Parameters	2D critical value (k_x)	1D critical value (k)
$c = 0.01$, $v = 0.01$	0.27	0.27
$c = 0.05$, $v = 0.05$	0.32	0.32
$c = 0.1$, $v = 0.1$	0.34	0.34
$c = 0.2$, $v = 0.2$	0.37	0.36

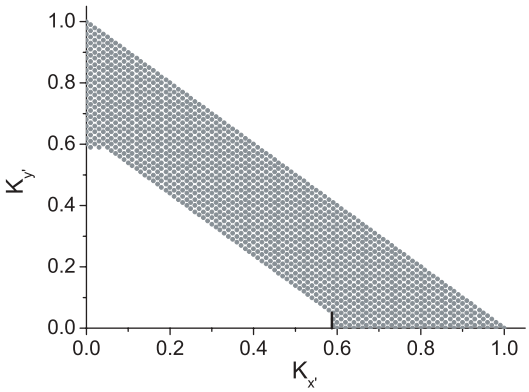

FIG. 4. Dynamical instability phase diagram in the rotated x'-y' coordinates for $c = 0.05$, $v = 0.05$. The marked border near $k'_x = 0.6$ corresponds to the section perpendicular to the diagonal line in Fig. 3.

C. Tight-binding approximation

We consider again the situation of strong lattice potential in which the tight-binding approximation works and an explicit result is obtained. By solving the eigenequation of $\sigma_z M$, we find the condition for dynamical instability

$$-\frac{\chi}{2K} < \sin^2(\pi q_x)\cos 2\pi k_x + \sin^2(\pi q_y)\cos 2\pi k_y < 0\,. \tag{27}$$

When this inequality is violated for any q_x, q_y, dynamical instability occurs, As a result, the boundary of dynamical instability is simply at $k_x = \frac{1}{4}, k_y = \frac{1}{4}$, which is the same as in the 1D case.

V. CONCLUSION

In the present work we have carried out extensive analytical and numerical analysis on Landau and dynamical instabilities for a BEC in a 2D optical lattice with the focus on the instability phase diagram and the property of the phase boundary. Our analytical results are able to provide understanding of many of salient features in our numerical results.

In a weak lattice, the criterion for the onset of Landau instability is similar to the classic Landau superfluid criterion: when the group velocity exceeds the sound velocity, the system becomes unstable against long-wavelength disturbance. This implies direction-independent behavior of the phase diagram boundary, as demonstrated in our numerical results. We have also found that the hydrodynamic analysis works for a wide range of parameters, including the tight-binding regime.

Our numerical results show that the shape of of the boundary of the dynamical instability phase diagram is nearly squarelike. Our analysis shows that this kind of shape is an indication that the 2D motion can be decomposed into two 1D motions.

Our theoretical results can be tested experimentally with BEC in moving 2D optical lattices. Finally, we stress that Landau instability and dynamical instability are universal phenomena in nonlinear periodic systems. Therefore, our results should also be very useful for other similar systems, such as nonlinear photonic crystals [44–46] and nonlinear waveguides [47–49].

ACKNOWLEDGMENTS

We thank Yongping Zhang for useful discussions. This work was supported by the "BaiRen" program of the Chinese Academy of Sciences, the NSF of China (10825417), and the MOST of China (2005CB724500, 2006CB921400).

APPENDIX: A PROOF

Since the appearance of complex eigenvalues of $\sigma_z M$ means that M is no longer positive definite [27], we assume all the eigenvalues are real. In this appendix we shall prove that $M_{\vec{k}}(\vec{q})$ is positive definite for all $\vec{q}$ if all eigenvalues of $\sigma_z M_{\vec{k}}(\vec{q})$ for the phonon modes are real and positive.

We consider the eigenequation

$$\sigma_z M(\vec{q})|X\rangle = \mu|X\rangle, \tag{A1}$$

with the phonon mode

$$\langle X|\sigma_z|X\rangle = (u, v)\sigma_z\begin{pmatrix} u \\ v \end{pmatrix} = 1. \tag{A2}$$

In the preceding and from now on all the subscripts are dropped for simplicity. We multiply both sides by σ_z and find

$$\langle X|M(\vec{q})|X\rangle = \mu\langle X|\sigma_z|X\rangle = \mu\,. \tag{A3}$$

This means that if $M(\vec{q})$ is positive definite, then the eigenvalue μ for the phone mode must be positive. Physically, this means that a phonon mode with negative μ can lower the energy of the system, leading to Landau instability.

We are now to prove that when all the eigenvalues of phonon modes of $\sigma_z M(\vec{q})$ are positive, $M(\vec{q})$ is positive definite for all $\vec{q}$. Denote the antiphonon mode as $|\widetilde{X}\rangle$ and its corresponding eigenvalue as $\tilde{\mu}$. Since $|X\rangle$ and $|\widetilde{X}\rangle$ form a complete orthogonal set, we can expand any vector as

$$|Y\rangle = \sum_n (a_n|X_n\rangle + b_n|\widetilde{X}_n\rangle). \tag{A4}$$

With this, we have

$$\begin{aligned}\langle Y|M(\vec{q})|Y\rangle &= \langle Y|\sigma_z\sigma_z M(\vec{q})|Y\rangle \\ &= \sum_n (|a_n|^2\mu_n - |b_n|^2\tilde{\mu}_n).\end{aligned} \tag{A5}$$

According to Ref. [27], if (u, v) is a phonon mode of $\sigma_z M(\vec{q})$ with eigenvalue μ, then (v^*, u^*) is an antiphonon mode of $\sigma_z M(-\vec{q})$ with $-\mu$. Therefore, if all the eigenvalues μ_n of $\sigma_z M(\vec{q})$ for phonon modes are positive, then all the eigenvalues $\tilde{\mu}_n$ for the antiphonon modes are negative. As a result, the right-hand side of Eq. (A5) is positive. This leads us to conclude that $\langle Y|M(\vec{q})|Y\rangle$ is positive for any vector $|Y\rangle$; therefore, $M(\vec{q})$ is positive definite for all $\vec{q}$. This completes our proof.

The implication of this proof is that $\sigma_z M(\vec{q})$ can also be used to determine the Landau instability other than $M(\vec{q})$, especially the onset of which. This mathematical result is certainly consistent with the well-accepted physics: When some phonon modes have negative excitations (corresponding to the eigenvalues in mathematics), they can lower the system energy, causing the Landau instability.

[1] O. Morsch and M. Oberthaler, Rev. Mod. Phys. **78**, 179 (2006).
[2] Y. Yukalov, Laser Phys. **19**, 1 (2009).
[3] B. P. Anderson and M. A. Kasevich, Science **282**, 1686 (1998).
[4] B. Wu and Q. Niu, Phys. Rev. A **64**, 061603(R) (2001).
[5] S. Burger, F. S. Cataliotti, C. Fort, F. Minardi, M. Inguscio, M. L. Chiofalo, and M. P. Tosi, Phys. Rev. Lett. **86**, 4447 (2001).
[6] C. Raman, M. Köhl, R. Onofrio, D. S. Durfee, C. E. Kuklewicz, Z. Hadzibabic, and W. Ketterle, Phys. Rev. Lett. **83**, 2502 (1999).
[7] R. Onofrio, C. Raman, J. M. Vogels, J. R. Abo-Shaeer, A. P. Chikkatur, and W. Ketterle, Phys. Rev. Lett. **85**, 2228 (2000).
[8] M. P. A. Fisher, P. B. Weichman, G. Grinstein, and D. S. Fisher, Phys. Rev. B **40**, 546 (1989).
[9] D. Jaksch, C. Bruder, J. I. Cirac, C. W. Gardiner, and P. Zoller, Phys. Rev. Lett. **81**, 3108 (1998).
[10] E. Altman, A. Polkovnikov, E. Demler, B. I. Halperin, and M. D. Lukin, Phys. Rev. Lett. **95**, 020402 (2005).
[11] K. W. Madison, F. Chevy, W. Wohlleben, and J. Dalibard, Phys. Rev. Lett. **84**, 806 (2000).
[12] M. Ben Dahan, E. Peik, J. Reichel, Y. Castin, and C. Salomon, Phys. Rev. Lett. **76**, 4508 (1996).
[13] K. Berg-Sørensen and K. Mølmer, Phys. Rev. A **58**, 1480 (1998).
[14] B. Wu and Q. Niu, Phys. Rev. A **61**, 023402 (2000).
[15] J. Liu, L. Fu, B.-Y. Ou, S.-G. Chen, D. I. Choi, B. Wu, and Q. Niu, Phys. Rev. A **66**, 023404 (2002).
[16] O. Morsch, J. H. Muller, M. Cristiani, D. Ciampini, and E. Arimondo, Phys. Rev. Lett. **87**, 140402 (2001).
[17] J. C. Bronski, L. D. Carr, B. Deconinck, J. N. Kutz, and K. Promislow, Phys. Rev. E **63**, 036612 (2001).
[18] V. V. Konotop and M. Salerno, Phys. Rev. A **65**, 021602(R) (2002).
[19] P. G. Kevrekidis and D. J. Frantzeskakis, Mod. Phys. Lett. B **18**, 173 (2004).
[20] M. Cristiani, O. Morsch, N. Malossi, M. Jona-Lasinio, M. Anderlini, E. Courtade, and E. Arimondo, Opt. Express **12**, 4 (2004).
[21] L. Fallani, L. De Sarlo, J. E. Lye, M. Modugno, R. Saers, C. Fort, and M. Inguscio, Phys. Rev. Lett. **93**, 140406 (2004).
[22] J. Mun, P. Medley, G. K. Campbell, L. G. Marcassa, D. E. Pritchard, and W. Ketterle, Phys. Rev. Lett. **99**, 150604 (2007).
[23] L. Khaykovich, F. Schreck, G. Ferrari, T. Bourdel, J. Cubizolles, L. D. Carr, Y. Castin, and C. Salomon, Science **296**, 1290 (2002).
[24] Y. P. Zhang and B. Wu, Phys. Rev. Lett. **102**, 093905 (2009).

[25] P. Noziéres and D. Pines, *The Theory of Quantum Liquids (II)* (Addison-Wesley, New York, 1990).
[26] B. Wu and J. R. Shi, e-print arXiv:cond-mat/0607098v2.
[27] B. Wu and Q. Niu, New J. Phys. **5**, 104 (2003).
[28] L. De Sarlo, L. Fallani, J. E. Lye, M. Modugno, R. Saers, C. Fort, and M. Inguscio, Phys. Rev. A **72**, 013603 (2005).
[29] A. Trombettoni and A. Smerzi, Phys. Rev. Lett. **86**, 2353 (2001).
[30] M. Krämer, L. Pitaevskii, and S. Stringari, Phys. Rev. Lett. **88**, 180404 (2002).
[31] M. Krämer, C. Menotti, L. Pitaevskii, and S. Stringari, Eur. Phys. J. D **27**, 247 (2003).
[32] A. J. Ferris, M. J. Davis, R. W. Geursen, P. B. Blakie, and A. C. Wilson, Phys. Rev. A **77**, 012712 (2008).
[33] M. Modugno, C. Tozzo, and F. Dalfovo, Phys. Rev. A **70**, 043625 (2004).
[34] Y. Zheng, M. Kostrun, and J. Javanainen, Phys. Rev. Lett. **93**, 230401 (2004).
[35] K. Iigaya, S. Konabe, I. Danshita, and T. Nikuni, Phys. Rev. A **74**, 053611 (2006).
[36] Z. X. Liang, X. Dong, Z. D. Zhang, and B. Wu, Phys. Rev. A **78**, 023622 (2008).
[37] A. Smerzi, A. Trombettoni, P. G. Kevrekidis, and A. R. Bishop, Phys. Rev. Lett. **89**, 170402 (2002).
[38] M. Machholm, C. J. Pethick, and H. Smith, Phys. Rev. A **67**, 053613 (2003).
[39] M. Machholm, A. Nicolin, C. J. Pethick, and H. Smith, Phys. Rev. A **69**, 043604 (2004).
[40] E. Taylor and E. Zaremba, Phys. Rev. A **68**, 053611 (2003).
[41] G. K. Campbell, J. Mun, M. Boyd, E. W. Streed, W. Ketterle, and D. E. Pritchard, Phys. Rev. Lett. **96**, 020406 (2006).
[42] K. Mølmer, New J. Phys. **8**, 170 (2006).
[43] K. M. Hilligsøe and K. Mølmer, Phys. Rev. A **71**, 041602(R) (2005).
[44] M. D. Iturbe-Castillo, M. Torres-Cisneros, J. J. Sánchez-Mondragón, S. Chávez-Cerda, S. I. Stepanov, V. A. Vysloukh, and G. E. Torres-Cisneros, Opt. Lett. **20**, 1853 (1995).
[45] A. V. Mamaev, M. Saffman, and A. A. Zozulya, Europhys. Lett. **35**, 25 (1996).
[46] M. I. Carvalho, S. R. Singh, and D. N. Christodoulides, Opt. Commun. **126**, 167 (1996).
[47] M. Stepić, C. Wirth, C. E. Rüter, and D. Kip, Opt. Lett. **31**, 247 (2006).
[48] J. Meier, G. I. Stegeman, D. N. Christodoulides, Y. Silberberg, R. Morandotti, H. Yang, G. Salamo, M. Sorel, and J. S. Aitchison, Phys. Rev. Lett. **92**, 163902 (2004).
[49] K. Tai, A. Hasegawa, and A. Tomita, Phys. Rev. Lett. **56**, 135 (1986).